Molecular Crystals and Liquid Crystals

Publication details, including instructions for authors and subscription information:
http://www.tandfonline.com/loi/gmcl16

Quasielastic Neutron Scattering and Orientational Motions in Liquid Crystals

C. J. Carlile [a] [b] & K. Krebs [a]

[a] Physics Division, Euratom C.C.R., Ispra (Varese), Italy

[b] Neutron Beam Research Unit, Rutherford Laboratory, Abingdon, England

To cite this article: C. J. Carlile & K. Krebs (1974): Quasielastic Neutron Scattering and Orientational Motions in Liquid Crystals, Molecular Crystals and Liquid Crystals, 29:1, 43-56

To link to this article: http://dx.doi.org/10.1080/15421407408083187

Mol. Cryst. Liq. Cryst., 1974, Vol. 29, pp. 43–56
© Gordon and Breach Science Publishers, Ltd.
Printed in Holland

Quasielastic Neutron Scattering and Orientational Motions in Liquid Crystals

C. J. CARLILE† and K. KREBS

Physics Division, Euratom C.C.R., Ispra (Varese), Italy

(*Received April 12, 1974; in final form July 24, 1974*)

The time scale of quasielastic slow neutron scattering (10^{-11}–10^{-12} sec) is such that one observes predominantly random motions of the atoms constituting a liquid crystal molecule with quasi-stationary centre of mass behaviour. Because of the high cross-section of hydrogen the observable modes are therefore reorientational jump motions of protons relative to the centre of mass. The quasielastic scattering from two liquid crystals was observed on an eleven-angle time-of-flight spectrometer at eleven temperatures. The samples used were *n*-(*p*-methoxybenzilidene)-*p*′-*n*-butylaniline (MBBA) and diethyl 4,4′-azoxydibenzoate (DAB) which exhibit nematic and smectic *A* mesophases respectively. The quasielastic broadening, represented by a single Lorentzian function of width ΔE is obtained from the raw data by a series of FORTRAN computer programs. The broadening curves of ΔE against momentum transfer squared, Q^2, exhibited a linear relationship which was analysed using a theory due to Larrson[20] giving a diffusion coefficient D_p describing the random change of the connection line between the scattering centre and the centre of mass, and a characteristic time τ_{00} representing a combination of the reorientational-vibrational period of the protons and the vibrational period of the molecular centre of mass. It is interesting to note that in the mesophases of both the nematic (MBBA) and the smectic (DAB) liquid crystal D_p remains constant with temperature. This probably reflects the compensation of the thermal activation of the directional axis motion by the ordering influence of the dispersion forces. Concerning τ_{00} we have found this remains constant in the nematic phase with a value in agreement with dielectric relaxation measurements[23] lending support to the theory that the individual molecules in nematic mesophases are rotating as single molecules. In contrast in the smectic *A* mesophase τ_{00} is highly temperature-dependent. We postulate that this is due to the rotation being collective in nature.

---

† Now at Neutron Beam Research Unit, Rutherford Laboratory, Abingdon, England.

INTRODUCTION

Research on liquid crystals has gained considerable interest in recent years due to their technological applications in opto-electronics and as thermo-optic devices. These substances are also of increasing importance for biophysical and biochemical studies. The existence of ordered mesostates points to the strong influence of intermolecular correlations in these liquids. Neutrons are a well known means to probe correlations. In the case of incoherent scattering one is able to measure the self-part of the correlation function or the behaviour of single molecules, and some results for neutron measurements have already been published.[1–5] Together with future neutron measurements on deuterated liquid crystals and in combination with optical scattering methods one has thus a powerful tool to study the dynamics of such systems which will be very essential for example in the understanding of biological membranes.

With slow neutron scattering the spatial observation range which is a few Å is determined by the momentum transfer Q. The observation times are of the order of 10^{-12} to 10^{-11} sec, which is quite different from other methods. Liquid crystals are mostly composed of elongated molecules. From measurements of their translational diffusion constants[6–8] one finds that the contribution to near elastic neutron scattering is probably of minor importance, in the normal range of Q available, thus on the time scale of quasielastic slow neutron scattering compared to the time scale of molecular motions in liquid crystals one observed predominantly single particle motion with quasi-stationary centre of mass behaviour. Because of the high cross section of hydrogen the remaining observable modes are motions of protons relative to the center of mass (c.o.m.). The present paper describes information we have obtained in this field by performing neutron measurements on both a nematic and a smectic liquid crystal.

EXPERIMENTAL METHOD

The dynamics of liquids is reflected in the Fourier components of their motional behaviour. These give rise to relatively large and continuous neutron energy distributions, thus a continuous observation method as is offered by the time-of-flight technique is most advantageous. The method also allows simultaneous measurements at many scattering angles to be performed affording an extended momentum transfer range.

The experiments described below have been made on a time-of-flight facility: the ISPRA-I Double Chopper Spectrometer[9] (Figure 1). The incident energy of the neutron beam was 6×10^{-3} eV and the resolution of the spec-

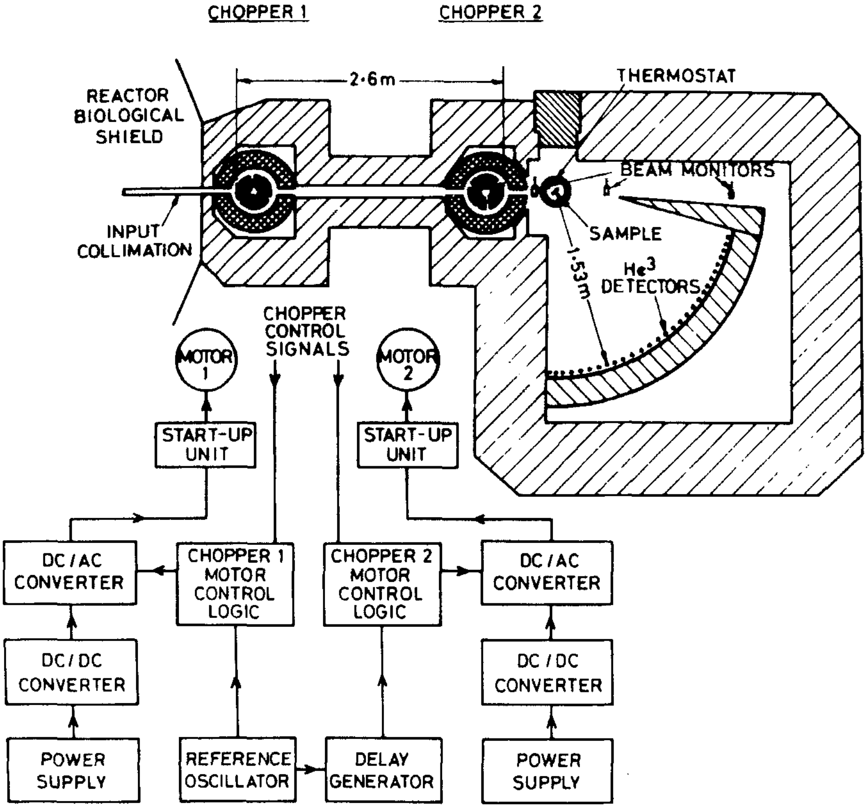

FIGURE 1 Double Chopper Spectrometer of the ISPRA-1 reactor

trometer was 7×10^{-4} eV. The two choppers constructed from a copper nickel alloy are each driven by a phase shifted reluctance motor. The power for each of these motors is supplied by a quartz stabilized thyristor based AC–DC converter unit. A digital electronic system controls and regulates permanently the phase shift between the two driving motors.[21] An exact control of the phase is a necessity for such measurements since on this depends the definition of the input energy and the possibility to observe small charges between the shape of the scattered spectrum and the spectrum obtained from a reference sample.

The two samples were *n*-(*p*-methoxy benzylidene)-*p*-*n*-butylaniline (MBBA)

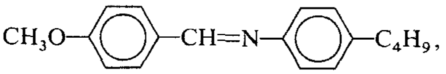

,

which exhibits a nematic mesophase within the range from 20°C to 41°C, obtained from Riedel-De Haen AG (Nr. 36320), and diethyl 4,4′-azoxydibenzoate (DAB)

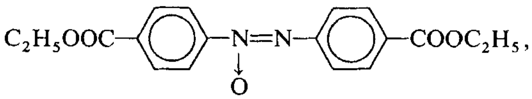

which exhibits a smectic *A* mesophase within the range of 114°C to 122°C, obtained from Eastman Kodak Co. (Nr. 9877).

A special aluminium holder containing a 1 mm thickness of the sample was enclosed in a double walled orientable aluminium thermostat unit by which the sample temperature was kept constant to within 0.2°C. The samples were not microscopically oriented by any external field and therefore the results correspond to an orientational average of the scattering over all molecular directions.

Scattered neutrons were detected by banks of He^3 counters, the direct beam being monitored by thin fission chambers. Data were collected and stored simultaneously from 11 detectors in an on-line PDP-8 computer using a specially developed time-of-flight decoder.[10,11] Much care was taken in the preparation of a set of FORTRAN data reduction programs for the IBM 370 computer. It is possible to combine the programs in such a manner as to produce the widths of the broadened quasielastic peaks in one step however it is advantageous to follow closely the development of the data and for this reason the data correction and analysis procedure was separated into three distinct steps utilising the specially written programs TOF, DOCHAP, and QUARKS. At any stage it is possible to detect any errors in the data reduction sequence which may have gone previously unobserved.

TOF transfers each data set, immediately after its collection, from paper tape into numerical and graphical hardcopy for inspection purposes and also into cards for the data input into DOCHAP. This step is effectively for the examination and preservation of raw data.

Each measurement of the sample was accompanied by a measurement on the empty aluminium sample holder as well as on a standard 10% scattering sample of vanadium. Thus three data sets are utilised as the input of the main data reduction program DOCHAP.[12] Basically this program performs a series of operations on the raw data, any one of which can be suppressed by means of a data switch card. These include: normalisation of the three data sets using beam monitor readings; flat background subtraction; time dependent background subtraction as determined by the holder spectrum; intercalibration of the efficiency of the separate detectors by means of the vanadium calibration spectrum; an air attenuation correction of the scattered beam; and a sample and vanadium thickness correction to take into account absorption or double scattering within the sample.[25] As the sample scattering was 15% of the incident beam no attempt was made to apply a more complete multiple scattering correction to the data as the effect on the experimental spectra of triple and higher order scattering will be less than 2% compared with typical statistical errors in the data points of 4% and in the final widths of 15%. Each time of flight spectrum is also corrected for the efficiency of the He^3 detectors as a function of energy. Finally a data smoothing option can be utilised to improve the statistical accuracy of the raw data. It must be emphasized that this option was always suppressed during the data reduction of these measurements so that the complete statistical error of the raw data would be preserved. The final output from this program is numerical and graphical hardcopy of the corrected data together with cards for the input of QUARKS.

The final aim of the data reduction chain is the production of quasi-elastic peak widths and intensities as a function of momentum transfer Q or scattering angle θ. This analysis is performed with the third program QUARKS which is an adaptation of a program originally developed at Birmingham University.[13] The intrinsic resolution function of the spectrometer is represented by the elastic peak of the vanadium standard for which no specific or analytical shape is assumed thus preserving the full information from each time-of-flight channel. Recent theories[22] have shown that the quasielastic broadening is a sum of a series of Lorentzians but the resolution of the spectrometer was sufficient to be able to resolve only one Lorentzian. The unresolved broader background under this function was, in a simplistic approach, assumed to be a straight line. An initial estimate of the energy broadening must be given as an input to QUARKS which convolutes the broadening function with the resolution function and by a multi-parameter Newton–Raphson χ^2 fitting procedure produces the best fit between the convoluted spectrum and the experimental data from the liquid crystal. The parameters which are varied by the program are:

1) the width ΔE of the Lorentzian,

2) the relative areas R of the two curves,

3) the shift Δt of the central channel of experimental and convoluted peaks, thereby taking into account any difference in the position of the sample and the vanadium in the incident beam,

4) the gradient A and,

5) the intercept B of the background beneath the convoluted curve.

In this way the statistical function χ^2 is reduced to a minimum, best fit values of the variable parameters are produced, and the experimental spectrum is fitted by a curve:

$$N(t) = R\left[\frac{\Delta E}{\Delta E^2 + \frac{m_N^2 L^4}{4}\left(\frac{1}{t^2} - \frac{1}{(t_0 + \Delta t)^2}\right)^2} + At + B\right]$$

convoluted with the resolution function of the spectrometer, where L is the flight path length and m_N is the mass of the neutron.

$N(t)$ is the count in a channel having a time-of-flight t, and t_0 is the central channel of the experimental spectrum. The main advantage of this method over previously used methods of extracting the broadening ΔE and intensity lies in the importance placed on each point of the quasielastic distribution and not just on its full width at half maximum as in the case of the calibration curve method[14] and the more restricted Voigt profile method. Because no smoothing of the raw data was carried out QUARKS, through the Newton-Raphson technique, produces a standard deviation on the final values which is directly related to the statistical error of the raw data. Examples of the goodness of fit to the experimental data are given in Figure 2.

EXPERIMENTAL RESULTS

On MBBA time-of-flight spectra have been measured for 11 scattering angles and for 11 temperatures T. After the complete data treatment as described in the above section the results are condensed into Figure 3, which indicates that the effective line broadening as a function of the momentum transfer is of the form

$$\Delta E(T) = a(T) + b(T)Q^2 \tag{1}$$

In the case of DAB spectra have been obtained for 11 scattering angles and for 9 temperatures. The corrected data are plotted in Figures 4 and 5 and again one sees that they follow a linear relationship. Due to the complete shut-down of the ISPRA-1 reactor it has been not possible to obtain sufficient data for the isotropic phase of DAB.

DISCUSSION

The larger size of the molecules, the observed translational diffusion constants and the general properties of liquid crystals indicate that at least at larger Q-values the observed broadening is mainly caused by atomic motions relative to their center of mass: thus we assume that orientational fluctuations predominate over density fluctuations with center of mass motions.

Several possibilities exist to describe these fluctuations of mainly orientational character. One might use a scheme which originally has been applied

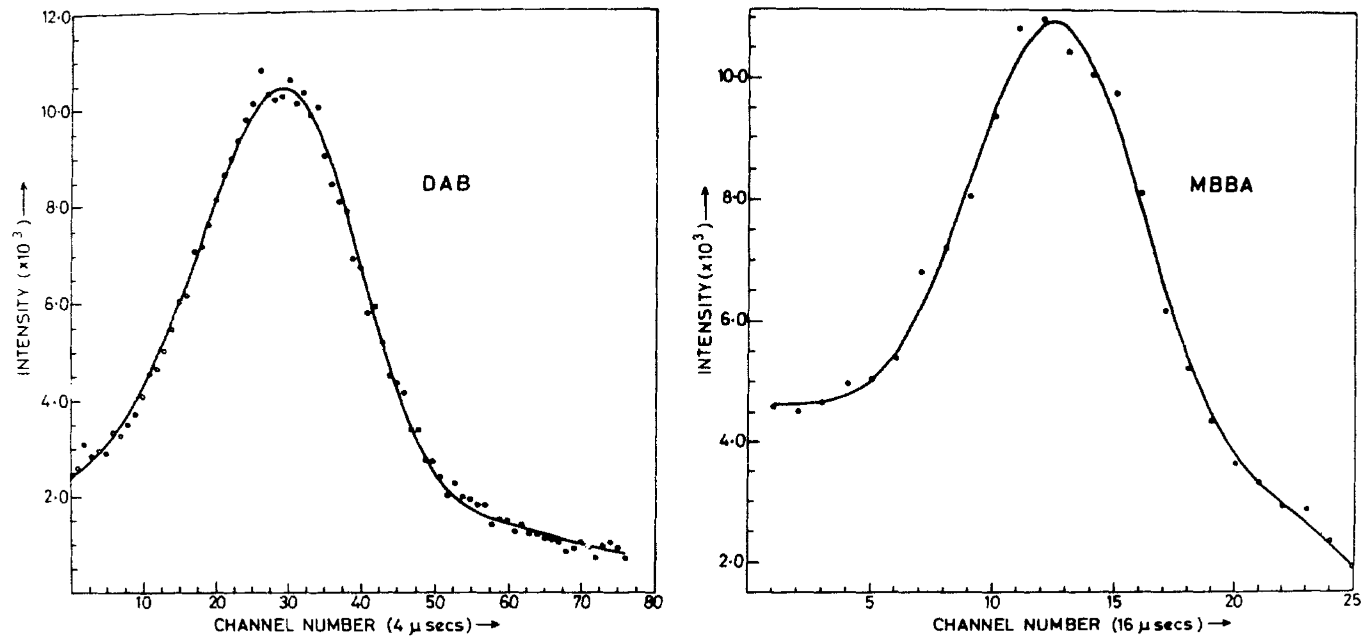

FIGURE 2 χ^2 fits of the convoluted resolution function to the experimental data. Left hand graph DAB, $\theta = 33.5°$, $T = 413$ K; right hand graph MBBA, $\theta = 80°$, $T = 308.5$ K. Points represent experimental data and continuous lines represent χ^2 fit.

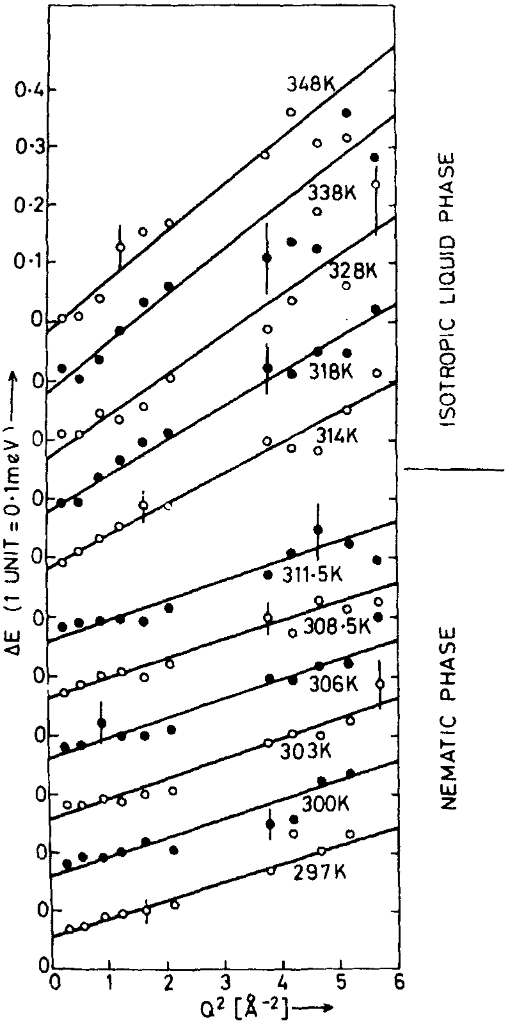

FIGURE 3 Broadening curves as a function of Q^2 for MBBA. Note the shift in origin of each curve. ● and ○ are used only for clarity. The lines are linear least-squares fits.

to the neutron scattering of rotating molecules.[15] In this case one has been able to calculate for a relatively general case the dependence of the width on the momentum transfer in the form of a reduced diagram. A parameter which can be obtained from this diagram is the rotational diffusion constant D_r. Applying this method one has found[16] for PAA values of the order of 10^{10} to 10^{11} sec^{-1}. However, this procedure should be considered with some reserve since the diagram mentioned above has been derived for the case of

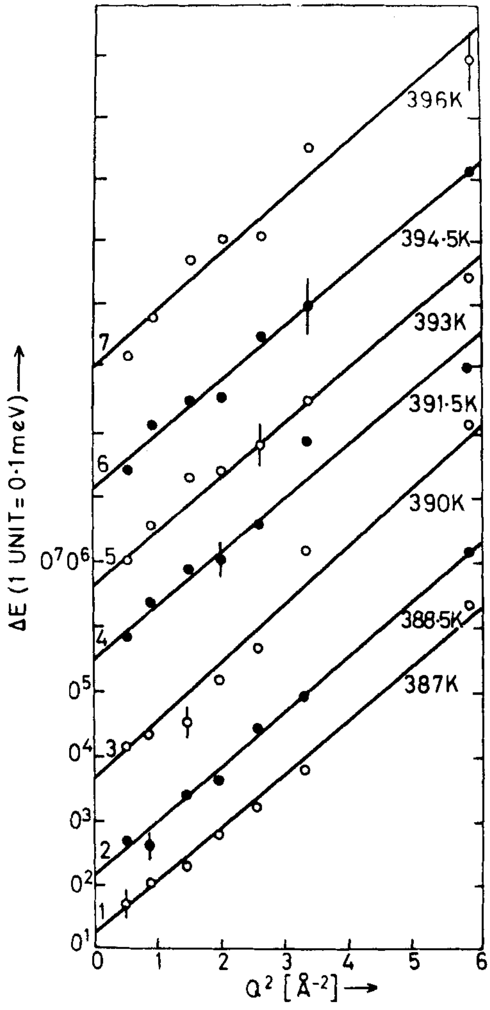

FIGURE 4 Broadening curves as a function of Q^2 for the smectic phase of DAB. 0^n represents the origin of curve *n*. ● and ○ are used only for clarity. The lines are linear least-squares fits.

spherical molecules and under the additional assumption that the isotropic forces on a molecule are much stronger than the anisotropic ones. Both considerations are certainly not characteristic for liquid crystals.

A second possibility[17,18] is based on the assumption that the liquid molecule performs vibrational motions occurring during a time τ_0 when the average orientation is not changing. This stationary time is then followed in a time τ_1 by a sudden orientational realignment which however must be small

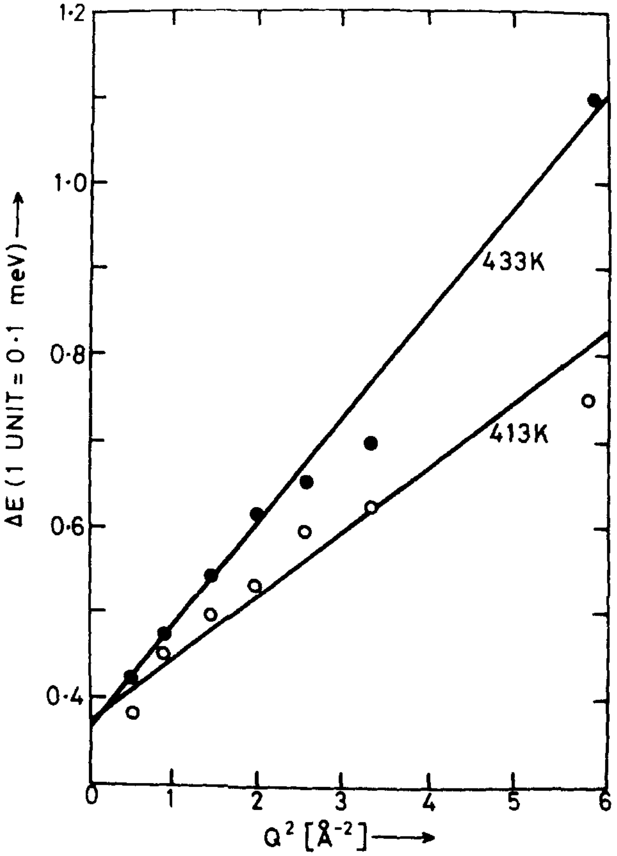

FIGURE 5 Broadening curves as a function of Q^2 for the isotropic liquid phase of DAB. The *lines are linear least-squares fits.*

due to the nature of the liquid crystalline state. In this case the following expression for the full width at half maximum of the quasielastic peak could be applied

$$\Delta E = 2\hbar\left(\frac{1}{\tau_0} + \frac{1}{\tau_0'}\right)(1 - F(Kr)\exp(-2W_T - 2W_R)) \tag{2}$$

where $2W_T$ is the Debye–Waller factor for c.o.m. oscillations and $2W_R$ the corresponding factor for rotational oscillations τ_0' is the time during which the c.o.m. of the molecule vibrates around a residence position. The $F(Kr)$ are related to rotational relaxation functions and defined by Larsson.[17] Formula (2) is valid under the assumption that c.o.m. vibrations predominate over c.o.m. diffusion, and that $\tau_0 \gg \tau_1$. Both assumptions seem quite plausible for liquid crystals. However, the disadvantage of Eq. (2) is the fact that its limiting behaviour at large Q values tends to a constant independent of Q. This is obviously in disagreement with our experimental finding as expressed by Eq. (1). Moreover there is also a difficulty with the large time behaviour of the rotational relaxation function.[19] As a third possibility[20] we consider the case in which the scattering protons perform vibrations relative to the c.o.m. simultaneously with small step changes of the average direction between the proton and the c.o.m. We believe that such a model is quite consistent with the dynamics of liquid crystals: in nematic liquids there exists a preferential average orientation which nevertheless still allows rotations around the long molecular axis, vibrational motions of end groups and also small changes of the molecular orientation. Therefore we base the interpretation of the experimental results on the formula:

$$\Delta E = 2\hbar\left(\frac{1}{\tau_0} + \frac{1}{\tau'_0} + \frac{2}{3}D_p Q^2\right) \tag{3}$$

In Equation (3) the following quantities have been introduced:

D_p = diffusion coefficient describing the gradual change of the connection line between the scattering centre and the c.o.m.,

τ_0 = diffusive-vibrational period of the protons with random small step changes of the connection line to the c.o.m.,

τ'_0 = vibratory period of c.o.m.

If we then identify the coefficient a of Eq. (1) with the quantity $2\hbar/\tau_{00}$ where $1/\tau_{00} = 1/\tau_0 + 1/\tau'_0$, and b with the coefficient $4\hbar D_p/3$ we obtain the values in Figures 6 and 7. It is interesting to note that in both cases D_p is independent of temperature within the ordered phase in agreement with earlier observations[1,4] on liquid crystals. This fact reflects probably the compensation of the thermal activation of the directional axis motion by the ordering influence of the dispersion forces. For the isotropic phase of MBBA the D_p-activation energy is 2.9 ± 0.8 kcal/mol, which is substantially lower than the values found for translational diffusion.[6,7]

Concerning τ_{00} for the case of MBBA we observe that in both the nematic and isotropic phases the period of the motion remains constant as a function of temperature. As the time scale in the nematic phase is in agreement with dielectric relaxation measurements[23] (25 ± 2 ps and 20.5 ps respectively) we can assume we are also seeing molecular rotation about the long axis of the molecule. The drop in relaxation time to 15 ± 2 ps in the isotropic liquid is presumably due to a smaller degree of molecular hindrance in the isotropic phase or perhaps to the contributions due to other motions, such as tumbling.

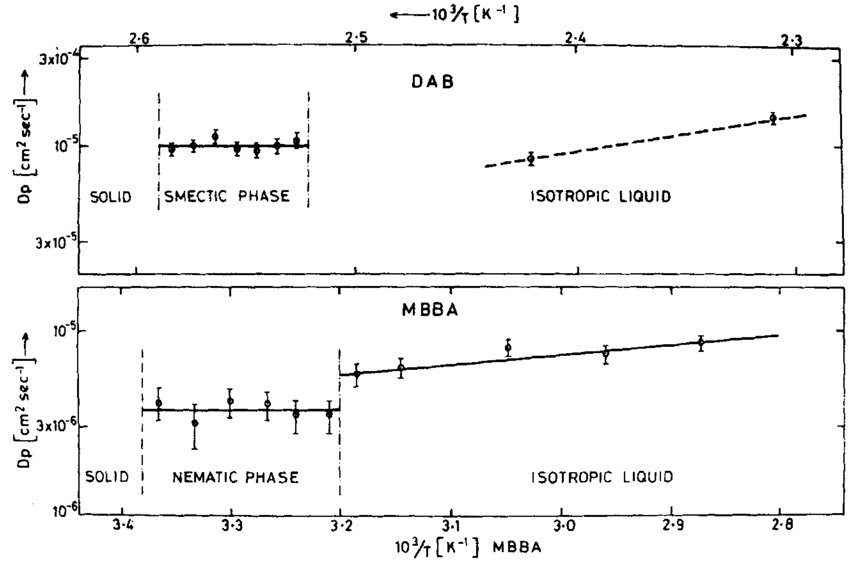

FIGURE 6 Diffusion constants D_p as a function of temperature for DAB and MBBA.

Turning now to the smectic *A* sample DAB we see again that the relaxation time remains constant in the isotropic phase and this is ascribed, as in the MBBA case, as being due to the body of the molecule rotating. However in the smectic *A* mesophase the relaxation time drops linearly with increasing temperature on an Arrhenius diagram. We postulate that this is because at the beginning of the smectic phase the body rotation is effectively frozen out because of the strong tranverse blocking effects due to the microscopic nature of the smectic *A* phase. As the temperature rises the barrier against rotation is overcome and body rotation occurs more freely. The activation energy for this mode is so high that we postulate many molecules are performing coupled collective rotations. Because of the relatively wide resolution function of the spectrometer it was not possible to distinguish the presumably faster rotations of the end groups of the molecules[24] which would give a very broad distribution merging in with the background.

CONCLUSION

We have obtained further evidence that the individual molecules in nematic mesophases are rotating, as a single molecule, and that the period of rotation remains constant. In contrast, in the smectic *A* mesophase, whilst the molecules are still rotating there is evidence to suggest that their rotation is collective in nature. The difference between the nematic and smectic *A*

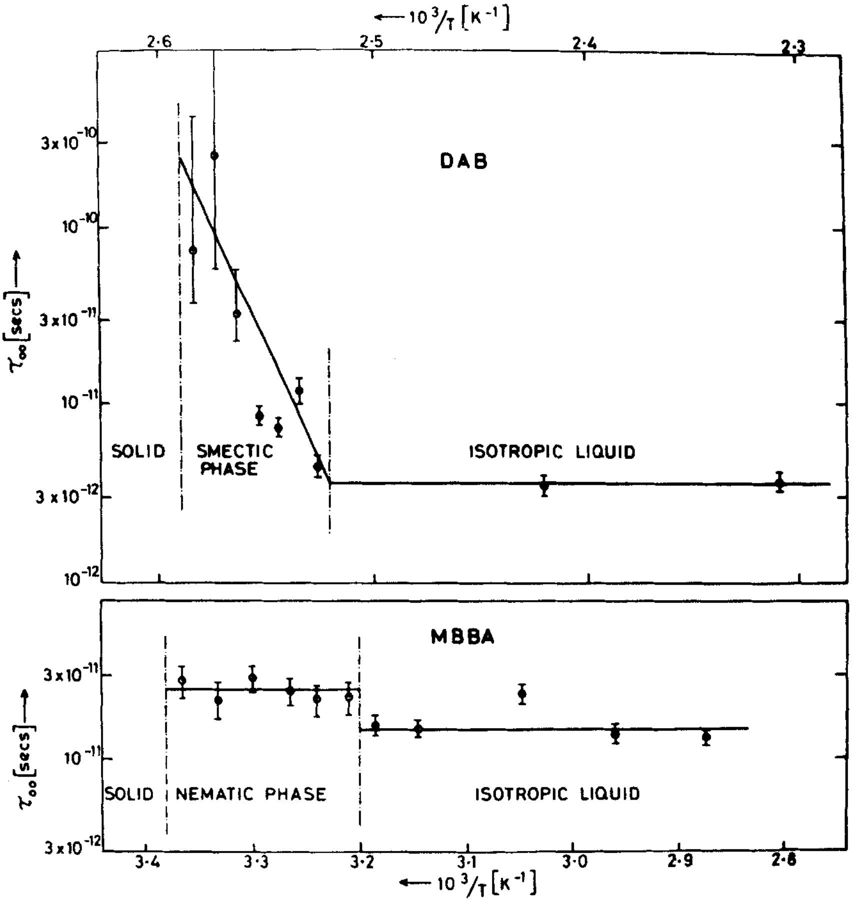

FIGURE 7 Combined residence times τ_{00} as a function of temperature for DAB and MBBA.

mesophases has been explained in terms of the microscopic differences between the two mesophases:

It is proposed to continue this work by performing further measurements, on a better resolution instrument, looking at a compound which exhibits both a smectic *A* and a nematic mesophase. In this way it is hoped that more quantitative conclusions regarding the motions of the molecules in the liquid crystal state can be reached.

Acknowledgements

We are pleased to acknowledge the competent technical help of W. Pütz. One of the authors (C.J.C) would like to thank the Commission of the European Communities for a fellowship to enable this work to be carried out.

References

1. R. Blinc and V. Dimic, *Phys. Lett.*, **31A**, 531 (1970).
2. R. Blinc, V. Dimic, J. Pirs, M. Vilfan, and I. Zupancic, *Mole. Cryst. Liq. Cryst.*, **14**, 97 (1971).
3. J. A. Janik, J. M. Janik, K. Otnes, and T. Riste, *Mole. Cryst. Liq. Cryst.*, **15**, 189 (1971).
4. K. Otnes, R. Pynn, J. A. Janik, and J. M. Janik, *Phys. Lett.*, **38A**, 335 (1972).
5. V. Dimic, L. Barbic, and R. Blinc, *Phys. Stat. Sol.* (*b*), **54**, 121 (1972).
6. S. K. Ghosh and E. Tettamanti, *Phys. Lett.*, **43A**, 361 (1973).
7. P. Martinoty, S. Candau, and F. Debeauvais, *Phys. Rev. Lett.*, **27**, 1123 (1971).
8. G. J. Krüger and H. Spiesecke, *Z. Naturforsch.*, **28A**, 964 (1973).
9. K. Krebs, *Neutron Inelastic Scattering*, II, p. 289, IAEA, Vienna (1968).
10. G. Colombo, N. Coppo, and L. Stanchi, *Nucl. Instr. Meth.*, **59**, 86 (1968).
11. H. J. Metzdorf, Euratom Report EUR 3933 e (1968).
12. K. Krebs and D. J. Winfield, Euratom Report EUR 4599 e (1971).
13. J. H. L. Birchall (unpublished).
14. D. J. Winfield, Euratom Report EUR 4516 e (1970).
15. P. A. Egelstaff, *J. Chem. Phys.*, **53**, 2590 (1970).
16. J. Töpler, B. Alefeld, and T. Springer, *Mole. Cryst. Liq. Cryst.* (in print).
17. K. E. Larsson, *Phys. Rev.*, **A3**, 1006 (1971).
18. A. Olivei, *Acta Cryst.*, **A29**, 692 (1973).
19. K. E. Larsson, *J. Chem. Phys.*, **59**, 4612 (1973).
20. K. E. Larsson, *Phys. Rev.*, **167**, 171 (1968).
21. J. Eder and D. Röbbelen, Euratom Report EUR 4881 e (1972).
22. See for example: T. Springer, *Springer Tracts in Physics*, **64**, 1 (1972).
23. P. Maurel and A. H. Price, *J. Chem. Soc. Far. Trans II*, **10**, 1486 (1973).
24. J. T. S. Andrews, *Phys. Letts.*, **46A**, 377 (1974).
25. C. J. Carlile, Rutherford Laboratory report RL-74-103 (1974).